

# Solitons in $\mathcal{PT}$ -symmetric systems with spin-orbit coupling and critical nonlinearity

Gennadiy Burlak<sup>1</sup>, Zhaopin Chen<sup>2\*</sup> and Boris A. Malomed<sup>3,4</sup>

<sup>1</sup>*Centro de Investigación en Ingeniería y Ciencias Aplicadas, Universidad Autónoma del Estado de Morelos, Cuernavaca, Morelos, Mexico*

<sup>2</sup>*Physics Department and Solid State Institute, Technion, Haifa 32000, Israel*

<sup>3</sup>*Department of Physical Electronics, School of Electrical Engineering, Faculty of Engineering, and Center for Light-Matter Interaction, Tel Aviv University, P.O.B. 39040, Tel Aviv, Israel*

<sup>4</sup>*Instituto de Alta Investigación, Universidad de Tarapacá, Casilla 7D, Arica, Chile*

We construct families of one-dimensional (1D) stable solitons in two-component  $\mathcal{PT}$ -symmetric systems with spin-orbit coupling (SOC) and quintic nonlinearity, which plays the critical role in 1D setups. The system models light propagation in a dual-core waveguide with skewed coupling between the cores. Stability regions for the solitons are identified in the system's parameter space. They include the main semi-infinite gap, and an additional finite *annex gap*. Stability boundaries are identified by means of simulations of the perturbed evolution, which agree with results produced by the linear-stability analysis for small perturbations. Distinct evolution scenarios are identified for unstable solitons. Generally, they suffer blowup or decay, while weakly unstable solitons transform into breathers. Due to a regularizing effect of SOC, stationary solitons are also found beyond the exceptional point, at which the  $\mathcal{PT}$  symmetry breaks down, but they are unstable. Interactions between adjacent solitons are explored too, featuring rebound or merger followed by blowup. Slowly moving (tilted) solitons develop weak oscillations, while fast ones are completely unstable. Also considered is the reduced diffractionless system, which creates only unstable solitons.

## I. INTRODUCTION

The current work in the field of optics has drawn a great deal of interest to using photonic media for emulation of various effects known in condensed-matter and quantum physics, where direct experimental and theoretical studies of such effects may be much more challenging. In many cases, the photonic emulation is facilitated by the fact that the universal equation of Schrödinger type, which governs the paraxial light propagation in linear and nonlinear media, is quite similar to the fundamental Schrödinger equation in quantum systems [1]. The similarity may be also established between Hamiltonians of the condensed-matter or quantum settings and effective Hamiltonians modeling optical phenomena.

Well-known examples of the emulation of diverse physical phenomenology by photonics are provided by the Hall effect [2], topological insulators [3], black holes [4],  $\mathcal{PT}$  (parity-time) symmetry [5], which was realized theoretically [6]-[13] and experimentally [14-16] in diverse optical setups, and (pseudo-) spin-orbit coupling (SOC) [17-19]. Photonic SOC schemes were designed to simulate SOC in atomic Bose-Einstein condensates (BECs) [20]-[24], which, in turn, was devised as the emulation of the SOC effect per se, which plays a major role in physics of semiconductors [25, 26].

$\mathcal{PT}$ -symmetric schemes are built as ones which include symmetrically placed and mutually balanced gain and loss elements, that makes it possible to produce stable excitation spectra [5], provided that the strength of the gain-loss terms does not exceed a certain critical value, which is often called the exceptional point [27-29]. In particular,  $\mathcal{PT}$  symmetry can be realized in *couplers*, i.e., dual-core optical waveguides with linear coupling between the cores [30-32]. In this case, one core of the  $\mathcal{PT}$ -symmetric coupler carries the gain, while the mate one provides the balancing loss [33-39].

As concerns SOC in BEC, it is modeled by systems of Gross-Pitaevskii equations for a spinor (two-component) wave function, coupled by linear terms with first spatial derivatives [21-23]. Accordingly, photonic emulation of such setups may be provided by an optical coupler, in which amplitudes of the electromagnetic fields in the two parallel cores correspond to the components of the BEC spinor wave function [18, 19, 40]. The aforementioned first derivatives are then provided either by temporal dispersion of the inter-core coupling constant in spatiotemporal optical couplers [18], or by spatial shear between two cores of the dual waveguide (its *skewness*) [19, 40].

Both  $\mathcal{PT}$  symmetry and SOC being linear phenomena, it is natural to consider their interplay. Dual-core waveguides, maintaining these phenomena in essentially the same system, offer an optical platform for integrating them.

---

\*Electronic address: zhaopin.chen@campus.technion.ac.il

Furthermore, the same setup allows one to add intrinsic nonlinearity of the waveguiding cores to the system, which opens the way to construct solitons and consider other nonlinear effects [19]. In particular, it is especially interesting to consider the case of the critical nonlinearity, which may give rise to the *critical collapse*. It occurs in two- or one-dimensional (2D or 1D) nonlinear Schrödinger/Gross-Pitaevskii equations with the cubic or quintic self-focusing, respectively [41–43]. Accordingly, solitons produced by these equations, i.e., 2D *Townes solitons* [44] and their 1D counterparts [45, 46], are unstable solutions (stability of multidimensional solitons, including ones with embedded vorticity, may be provided by the quadratic, i.e., second-harmonic-generating, nonlinearity [47]). In line with these well-known results, it was commonly believed that 2D systems with cubic self-focusing in free space always produce unstable solitons [48]. Nevertheless, in work [49] it was demonstrated that the linear SOC terms, added to the 2D system, make it possible to produce completely stable solitons of two types, *viz.*, semi-vortices and mixed modes, which play the role of the system’s ground state. Then, it was demonstrated that the emulation of SOC in the 1D dual-core coupler with the quintic self-focusing creates stable solitons, instead of collapsing ones, in this case as well [40].

The interplay of the  $\mathcal{PT}$  symmetry and critical (cubic) self-focusing in the presence of SOC in the 2D coupler, studied in the presence of the optically-emulated SOC [19], is quite interesting because, while the combination of the  $\mathcal{PT}$ -symmetric gain-loss terms and critical nonlinearity makes the solitons fragile states, the SOC terms secure their stability. The objective of the present work is to address a similar problem in 1D, i.e., in the system of nonlinear-Schrödinger equations modeling the dual-core optical waveguide with the gain, loss, and quintic self-focusing in the two cores, which are coupled by the above-mentioned skewed linear terms. The result is that vast families of *stable solitons* exist in this system. Boundaries of the stability areas are identified in the system’s parameter space.

The subsequent presentation is arranged as follows. The model of the nonlinear  $\mathcal{PT}$ -symmetric coupler, which provides the optical emulation of SOC, is formulated in Section II. It includes both the full system and a reduced one, which neglects the terms representing the paraxial diffraction in the dual-core coupler. The same section presents linearized equations necessary for the analysis of the solitons’ stability, and an approximate analytical solution for the solitons in the case when both the  $\mathcal{PT}$  symmetry and SOC may be treated as weak perturbations. Numerical results are reported in Section III. They include stability areas for solitons in the system’s parameter space and results of systematic numerical simulations for the evolution of unstable solitons (in particular, weakly unstable solitons may avoid the collapse, transforming, instead, into breathers or tilted (slowly moving) modes). Unlike the full system, the reduced one produces solely unstable solitons. Interactions between stable solitons are also studied by means of systematic simulations. The paper is concluded by Section IV.

## II. THE MODELS

Generalizing the considerations presented in Refs. [18, 19] and [40], the interplay of the (pseudo-) SOC, critical nonlinearity, and  $\mathcal{PT}$  symmetry in the 1D setting may be realized in the planar dual-core waveguide modeled by the following system of linearly-coupled nonlinear Schrödinger equations for complex amplitudes  $u(x, z)$  and  $v(z, x)$  of optical fields in the two cores:

$$\begin{aligned} iu_z + \frac{1}{2}u_{xx} + |u|^4u + v - \delta \cdot v_x &= i\gamma u, \\ iv_z + \frac{1}{2}v_{xx} + |v|^4v + u + \delta \cdot u_x &= -i\gamma v. \end{aligned} \quad (1)$$

Here  $z$  and  $x$  are, respectively, the scaled propagation distance and transverse coordinate, coefficients of the paraxial diffraction, quintic self-focusing, and straight inter-core coupling are scaled to be 1, real  $\delta > 0$  represents the inter-core shear in the skewed coupler, and  $\gamma > 0$  is the strength of the  $\mathcal{PT}$ -symmetric gain and loss terms.

In physical units, the  $x = 1$  and  $z = 1$  in Eqs. (1) and (2) correspond to  $\sim 50 \mu\text{m}$  and 1 cm, respectively. Assuming the use of optical materials which feature strong quintic nonlinearity [50], an estimate of the power of laser beams which are required to create the solitons considered below yields  $\sim 10 \text{ kW}$ , the respective power density being  $\sim 10 \text{ GW/cm}^2$ .

In the absence of the gain and loss ( $\gamma = 0$ ), Eqs. (1) and (2) conserve the total power (norm) and momentum of the wave field,

$$P = \int_{-\infty}^{+\infty} (|u(x)|^2 + |v(x)|^2) dx, \quad M = i \int_{-\infty}^{+\infty} (u_x^* u + v_x^* v) dx. \quad (3)$$

with  $*$  standing for the complex conjugate. The  $\mathcal{PT}$  terms break the conservation, giving rise to the following evolution

equations for the power and momentum:

$$\frac{dP}{dz} = 2\gamma \int_{-\infty}^{+\infty} (|u|^2 - |v|^2) dx, \quad (4)$$

$$\frac{dM}{dz} = 2i\gamma \int_{-\infty}^{+\infty} (u_x^* u - v_x^* v) dx. \quad (5)$$

Stationary solutions of Eqs. (1) and (2) with real propagation constant  $k$  are looked as

$$\{u, v\} = e^{ikz} \{U(x), V(x)\}. \quad (6)$$

The corresponding equations for complex functions  $U(x)$  and  $V(x)$  are

$$-kU + \frac{1}{2} \frac{d^2 U}{dx^2} + |U|^4 U + V - \delta \cdot \frac{dV}{dx} = i\gamma U, \quad (7)$$

$$-kV + \frac{1}{2} \frac{d^2 V}{dx^2} + |V|^4 V + U + \delta \cdot \frac{dU}{dx} = -i\gamma V. \quad (8)$$

It is relevant to identify the spectrum of the linearized system. Looking for small-amplitude solutions to Eqs. (7) and (8) in the form of plane waves,

$$\{U, V\} \sim \exp(iqx), \quad (9)$$

with wavenumber  $q$ , one derives the following dispersion relation between  $k$  and  $q^2$ :

$$k = -(1/2)q^2 \pm \sqrt{1 - \gamma^2 + \delta^2 q^2}. \quad (10)$$

The spectrum is real, i.e., the  $\mathcal{PT}$  symmetry holds, under the condition of  $\gamma < 1$ , while  $\gamma = 1$  corresponds to the *exceptional point* [27–29] of the  $\mathcal{PT}$ -symmetric system. In terms of the dual-core system, the strengths of the straight inter-core coupling and gain-loss terms are exactly equal at this point.

At  $\gamma > 1$ , the  $\mathcal{PT}$  symmetry breaks down, and spectrum (10) becomes complex (unstable). It is relevant to note that, in the absence of SOC (at  $\delta = 0$ ), the entire spectrum blows up (immediately becomes complex) at any  $\gamma > 1$ . On the other hand, SOC provides a regularizing effect, as, at  $\gamma > 1$  and  $\delta \neq 0$ , spectrum (10) is complex only at sufficiently small wavenumbers, *viz.*, at

$$q^2 < (\gamma^2 - 1) / \delta^2. \quad (11)$$

It is shown below that, as a result of the regularization, Eqs. (7) and (8) may produce stationary soliton solutions at  $\gamma > 1$ , although those solutions are unstable, see Fig. 9 below.

Inversion of Eq. (10) yields  $q^2$  as a function of  $k$ :

$$q^2 = 2 \left( \delta^2 - k \pm \sqrt{\delta^4 - 2\delta^2 k + 1 - \gamma^2} \right). \quad (12)$$

It follows from Eq. (12) that solitons may populate the *semi-infinite bandgap* (SIG) of the system's spectrum, which is

$$k > k_{\text{SIG}} \equiv \frac{1}{2} \left( \delta^2 + \frac{1 - \gamma^2}{\delta^2} \right), \quad (13)$$

In the SIG, Eq. (12) gives rise to complex values of  $q$ , which implies that solitons, if they exist, feature exponentially decaying tails with spatial oscillations, such as  $\exp(-a|x|) \cdot \cos(bx)$ , with real constants  $a > 0$  and  $b$ . In addition to that, in the case of

$$\delta^4 < 1 - \gamma^2, \quad (14)$$

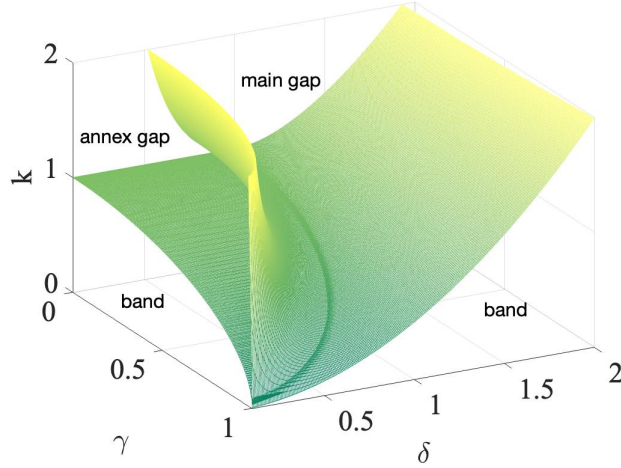


FIG. 1: (Color online.) The bandgap structure plotted according to the dispersion relation (12) and Eqs. (13)-(15).

there exists an extra finite *annex gap* (AG):

$$\sqrt{1 - \gamma^2} < k < \frac{1}{2} \left( \delta^2 + \frac{1 - \gamma^2}{\delta^2} \right), \quad (15)$$

cf. its counterpart for  $\gamma = 0$  obtained in Ref. [40]. In interval (15), Eq. (12) yields purely imaginary  $q$ , hence the solitons, if they populate the AG, have exponentially decaying tails without oscillations.

On the other hand, under condition

$$\delta^4 > 1 - \gamma^2, \quad (16)$$

SIG is the single bandgap, and the AG does not exist in this case.

The region of the existence of the gaps can be also defined in the plane of  $(\gamma, \delta)$  for fixed  $k$ . Indeed, it follows from Eqs. (13) that the SIG exists in the area defined by the system of inequalities

$$1 + \delta^4 - 2k\delta^2 \equiv \gamma_{\text{SIG}}^2 < \gamma^2 < 1, \quad (17)$$

In addition to it, the AG exists in the area defined by the following inequalities:

$$1 - k^2 < \gamma^2 < 1 - \delta^4. \quad (18)$$

At the exceptional point  $\gamma = 1$ , the AG does not exist, while the main SIG takes a simple form,

$$k > \delta^2/2. \quad (19)$$

In Fig. 1, the bandgap structure as a whole is displayed in the space of  $(\delta, \gamma, k)$ , see also Fig. 6 below.

Furthermore, for “moving” solitons (in fact, ones tilted in the spatial domain) Eqs. (1), (2) and (7), (8) can be rewritten in terms of  $z$  and the tilted coordinate,

$$\xi \equiv x - cz, \quad (20)$$

where  $c$  is the tilt (“velocity”). The resulting dispersion relation, including  $c$ , is rather cumbersome, but it takes a simple form at the exceptional point ( $\gamma = 1$ ), at which the SIG becomes

$$k > k_{\text{SIG}}(\gamma = 1, c) = (|c| + \delta)^2/2, \quad (21)$$

cf. Eq. (19). According to Eq. (21), the SIG decreases with the increase of  $|c|$ .

### A. Approximate soliton solutions

In the absence of the SOC terms ( $\delta = 0$ ), exact symmetric solitons produced by Eqs. (7) and (8) are obvious:

$$U_{\delta=0}(x) = \sqrt{\sqrt{1-\gamma^2} - i\gamma U_0(x; \gamma)}, \quad (22)$$

$$V_{\delta=0}(x) = \sqrt{\sqrt{1-\gamma^2} + i\gamma U_0(x; \gamma)}, \quad (23)$$

$$U_0(x; \gamma) = \frac{\left[3 \left(k - \sqrt{1-\gamma^2}\right)\right]^{1/4}}{\sqrt{\cosh\left(2\sqrt{2}\left(k - \sqrt{1-\gamma^2}\right)x\right)}}. \quad (24)$$

They exist for  $k > \sqrt{1-\gamma^2}$ , and are definitely unstable, for the same reason as the usual 1D Townes solitons, corresponding to  $\gamma = 0$  [45].

When both  $\gamma$  and  $\delta$  are small parameters, an approximate solution can be written as a straightforward extension of Eq. (43) from Ref. [40], where it was obtained, in a real form, for  $\gamma = 0$ :

$$U(x) \approx \left(1 - i\frac{\gamma}{2}\right) U_0(x; 0) - \frac{\delta}{2} \frac{dU_0(x; 0)}{dx}, \quad (25)$$

$$V(x) \approx \left(1 + i\frac{\gamma}{2}\right) U_0(x; 0) + \frac{\delta}{2} \frac{dU_0(x; 0)}{dx}. \quad (26)$$

Here,  $U_0$  is the expression given by Eq. (24).

### B. Equations for small perturbations

For the study of stability of solitons, perturbed solutions with complex eigenmodes of small perturbations,  $\phi_{1,2}(x)$  and  $\psi_{1,2}(x)$ , are introduced as

$$u = e^{ikz} [U(x) + \exp(\sigma z) \phi_1(x) + \exp(\sigma^* z) \phi_2^*(x)], \quad (27)$$

$$v = e^{ikz} [V(x) + \exp(\sigma z) \psi_1(x) + \exp(\sigma^* z) \psi_2^*(x)], \quad (28)$$

where  $U(x)$  and  $V(x)$  represent the unperturbed solution, and  $\sigma$  is the instability growth rate (it may be complex). The resulting problem for eigenmodes amounts to the linearized system of equations derived by the substitution of expressions (27) and (28) in Eqs. (1) and (2):

$$\begin{aligned} (-k + i\sigma - i\gamma) \phi_1 + \frac{1}{2} \frac{d^2 \phi_1}{dx^2} + 3|U(x)|^4 \phi_1 + 2|U(x)|^2 (U(x))^2 \phi_2 + \psi_1 - \delta \frac{d\psi_1}{dx} &= 0, \\ (-k - i\sigma + i\gamma) \phi_2 + \frac{1}{2} \frac{d^2 \phi_2}{dx^2} + 3|U(x)|^4 \phi_2 + 2|U(x)|^2 (U^*(x))^2 \phi_1 + \psi_2 - \delta \frac{d\psi_2}{dx} &= 0, \\ (-k + i\sigma + i\gamma) \psi_1 + \frac{1}{2} \frac{d^2 \psi_1}{dx^2} + 3|V(x)|^4 \psi_1 + 2|V(x)|^2 (V(x))^2 \psi_2 + \phi_1 + \delta \frac{d\phi_1}{dx} &= 0, \\ (-k - i\sigma - i\gamma) \psi_2 + \frac{1}{2} \frac{d^2 \psi_2}{dx^2} + 3|V(x)|^4 \psi_2 + 2|V(x)|^2 (V^*(x))^2 \psi_1 + \phi_2 + \delta \frac{d\phi_2}{dx} &= 0. \end{aligned} \quad (29)$$

As usual, the solitons are stable if all eigenvalues  $\sigma$  have  $\text{Re}(\sigma) \leq 0$ .

### C. The reduced system

Following Refs. [19] and [40], it is interesting to consider the reduced version of the system for broad solitons, in which the diffraction terms (second derivatives) may be omitted. In this case, rescaling makes it possible to fix  $\delta \equiv 1$ ,

and Eqs. (1), (2) and (7), (8) are replaced, respectively, by

$$iu_z + |u|^4 u + v - v_x = i\gamma u, \quad (30)$$

$$iv_z + |v|^4 v + u + u_x = -i\gamma v, \quad (31)$$

$$-kU + |U|^4 U + V - \frac{dV}{dx} = i\gamma U, \quad (32)$$

$$-kV + |V|^4 V + U + \frac{dU}{dx} = -i\gamma V. \quad (33)$$

In this case, dispersion relation (10) is replaced by

$$k = \pm \sqrt{1 - \gamma^2 + q^2}. \quad (34)$$

The condition of the  $\mathcal{PT}$  symmetry keeps the same form as above,  $\gamma < 1$ . In this case, Eq. (34) gives rise to a finite bandgap, unlike the SIC generated by the full system,

$$|k| < \sqrt{1 - \gamma^2}. \quad (35)$$

Note that, at the exceptional point  $\gamma = 1$ , dispersion relation (34) takes the form of the *Dirac's cone*,  $k = \pm|q|$ , with bandgap (35) shrinking to nil.

It is relevant to mention that, by means of substitution  $u = A + iB$ ,  $v = iA + B$ , the linear version of Eqs. (30) and (31) can be transformed into the spinor  $\mathcal{PT}$ -symmetric system for fields  $A$  and  $B$ , which was introduced in Ref. [51].

In the absence of the gain and loss ( $\gamma = 0$ ), it is straightforward to find exact real solutions to Eqs. (32) and (33), extending the method elaborated in Ref. [19] for effectively the same system, but with the cubic nonlinearity. The exact solution is

$$\begin{aligned} \{U(x), V(x)\} &= A(x) \{\cos \theta(x), \sin \theta(x)\}, \\ A^4(x) &= 12 \frac{k - \sin(2\theta(x))}{4 - 3 \sin^2(2\theta(x))}, \\ \theta(x) &= -\frac{\pi}{4} + \arctan \left[ \frac{1+k}{\sqrt{1-k^2}} \tanh \left( 2\sqrt{1-k^2}x \right) \right]. \end{aligned} \quad (36)$$

In Ref. [40] it was produced only in an approximate form. Although the solution (36) is completely unstable in the framework of Eqs. (30) and (31), the instability is weak, i.e., the solution is a physically relevant one, for  $0 < 1+k \ll 1$  [40].

As concerns the “moving” (tilted) solutions, for which Eqs. (30), (31) and (32), (33) should be rewritten in terms of  $z$  and moving coordinate (20), the accordingly modified dispersion relation (34) is

$$k = -cq \pm \sqrt{1 - \gamma^2 + q^2}. \quad (37)$$

It gives rise to a narrower gap, in comparison with one (35):

$$|k| < \sqrt{(1-c^2)(1-\gamma^2)}, \quad (38)$$

provided that  $c^2 < 1$ . In the case of  $c^2 > 1$ , gap (38) does not exist.

The stability of stationary solutions to Eqs. (30) and (31) can be explored using the same ansatz (27), (28) as introduced above. The corresponding linearized equations for the perturbation eigenmodes are obtained from Eqs.

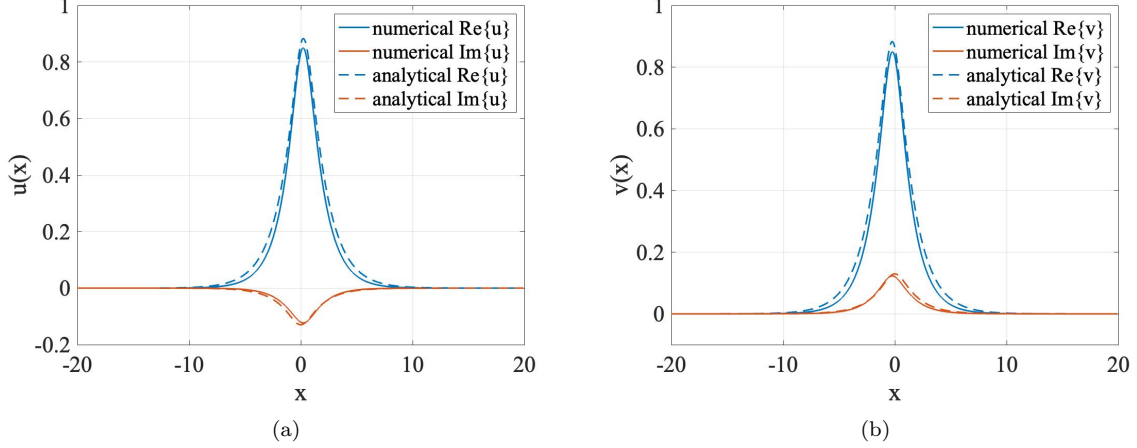


FIG. 2: (Color online). Numerically found components of a stable soliton with  $\delta = 0.35$ ,  $\gamma = 0.3$ , and  $k = 1.14$ , and their counterparts produced by the analytical approximation based on Eqs. (25) and (26).

(29) by dropping the second derivatives:

$$\begin{aligned}
 (-k + i\sigma - i\gamma) \phi_1 + 3 |U(x)|^4 \phi_1 + 2 |U(x)|^2 (U(x))^2 \phi_2 + \psi_1 - \frac{d\psi_1}{dx} &= 0, \\
 (-k - i\sigma + i\gamma) \phi_2 + 3 |U(x)|^4 \phi_2 + 2 |U(x)|^2 (U^*(x))^2 \phi_1 + \psi_2 - \frac{d\psi_2}{dx} &= 0, \\
 (-k + i\sigma + i\gamma) \psi_1 + 3 |V(x)|^4 \psi_1 + 2 |V(x)|^2 (V(x))^2 \psi_2 + \phi_1 + \frac{d\phi_1}{dx} &= 0, \\
 (-k - i\sigma - i\gamma) \psi_2 + 3 |V(x)|^4 \psi_2 + 2 |V(x)|^2 (V^*(x))^2 \psi_1 + \phi_2 + \frac{d\phi_2}{dx} &= 0.
 \end{aligned} \tag{39}$$

### III. NUMERICAL RESULTS

#### A. The stability chart for soliton families

Stationary soliton solutions of Eq. (7) and (8) were obtained by means of the squared-operator iteration method [52, 53]. Then, their stability was identified through the set of eigenvalues produced by a numerical solution of linearized equations (29), and verified by simulations of Eqs. (1) and (2) for perturbed evolution of the solitons, using the split-step Fourier method. The numerical solutions were constructed, chiefly, in the domain of size  $|x| \leq 20$ , covered by a numerical mesh of 512 sites, with absorbing boundary conditions.

First, Fig. 2 shows good agreement of the analytical approximation, given by Eqs. (25) and (26), with a numerical solution obtained for a moderately small value of  $\delta$  and small  $\gamma$ . Additional examples of stable and unstable numerically found solitons are shown in Figs. 3 and 4. In particular, the analytical approximation correctly predicts splitting  $\Delta x \simeq \delta$  between peaks of the linearly coupled components.

It is relevant to mention the system also support  $\mathcal{PT}$ -antisymmetric solitons, but they are all strongly unstable, similar to what is known in many other  $\mathcal{PT}$ -symmetric systems [54–57]. A typical example is displayed in Fig. 5.

In addition to the symmetric and antisymmetric modes, the conservative system with  $\gamma = 0$  admits asymmetric solutions [40]. However, in the case of  $\gamma \neq 0$  asymmetric states does not exist, as they cannot maintain the balance between the gain and loss.

The results are summarized in Fig. 6, which displays numerically found stability boundaries for soliton families in the plane of the gain-loss and SOC coefficients,  $(\gamma, \delta)$ , for several fixed values of the propagation constant  $k$ . The figure also includes the boundary between the SIG and band of linear waves, in which solitons cannot exist. This boundary is determined by Eq. (15), while the boundary between the SIG and AG is given by Eq. (17).

The stability border was eventually identified according to results of direct simulations of solitons with random noise at the amplitude level of 1% added to the input. The simulations were run over the propagation distance

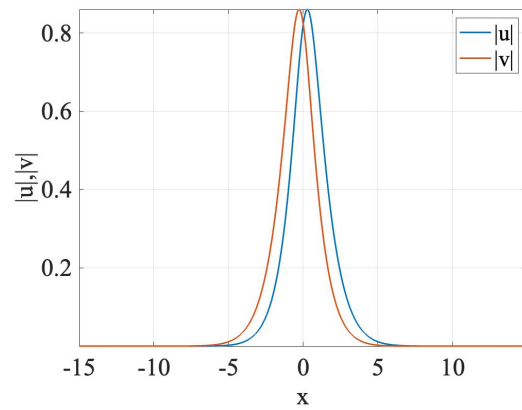


FIG. 3: (Color online). A typical example of a stable soliton in the system with  $\delta = 0.8, \gamma = 0.1$ , corresponding to the propagation constant  $k = 1.2$ . This soliton is stable in terms of eigenvalues of small perturbations and direct simulations of the perturbed evolution.

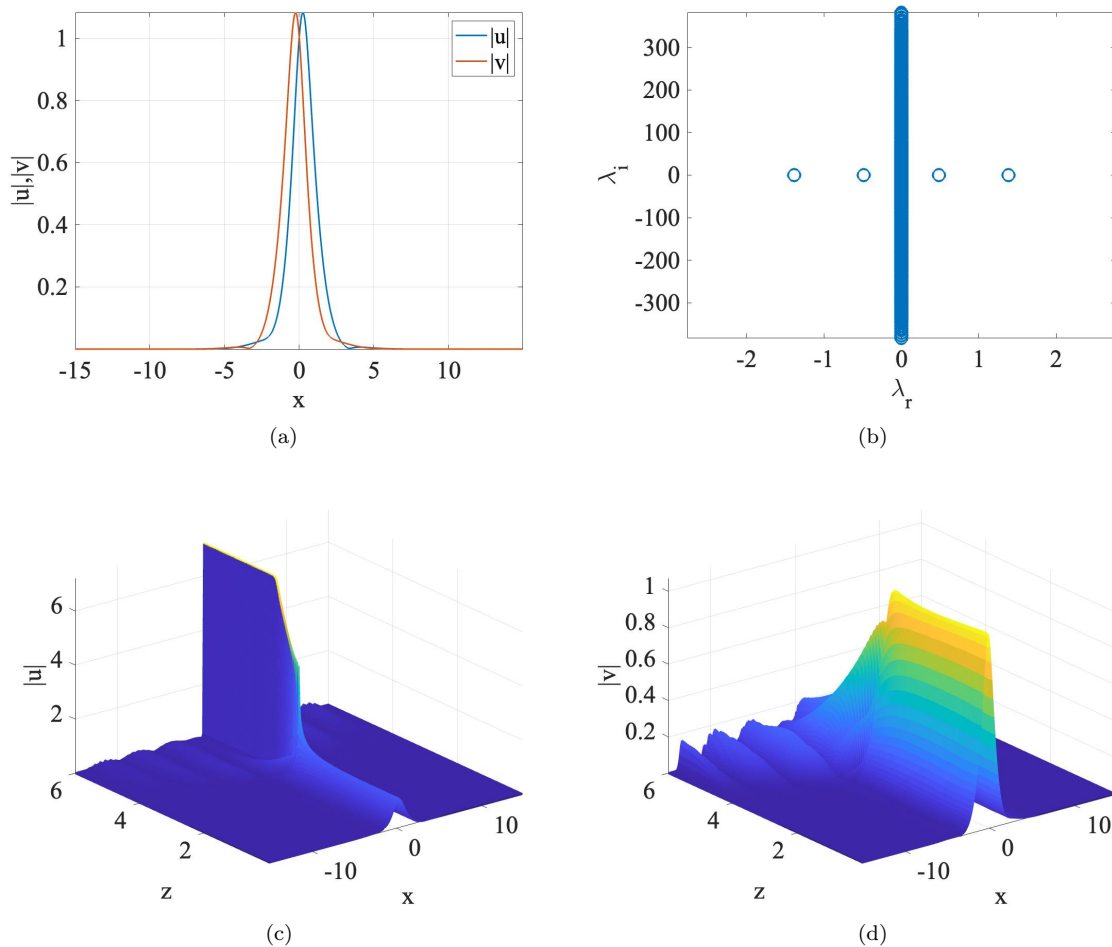


FIG. 4: (Color online). A typical example of an unstable soliton in the system with  $\delta = 0.8, \gamma = 0.8$  for  $k = 1.2$ . (a) The shape of the soliton; (b) the spectrum of eigenvalues for small perturbations, including unstable ones; (c) and (d) the evolution of the soliton under the action of a small random perturbation at the amplitude level of 1%. Eventually, one component of the soliton blows up and the other one decays. In (c), the growth of the amplitude is limited by the numerical scheme.

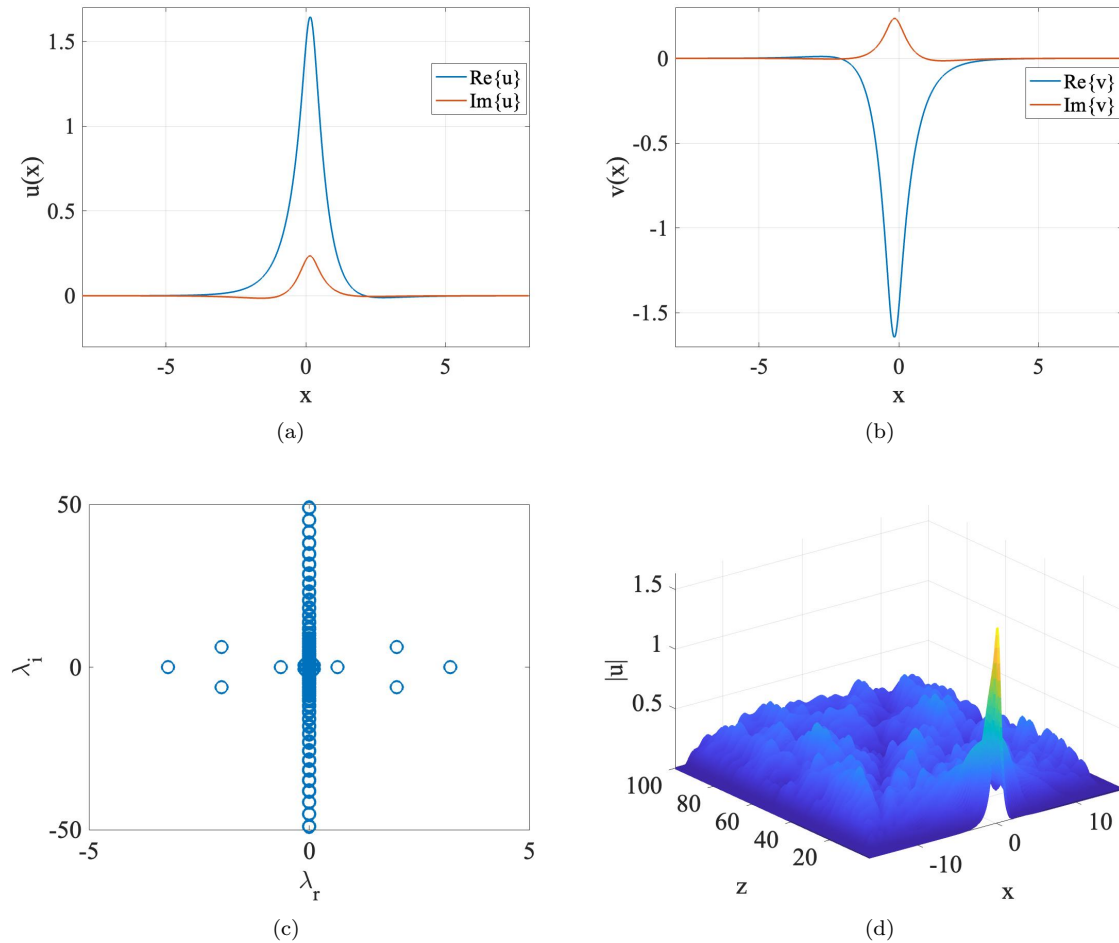


FIG. 5: (Color online). A typical example of an unstable  $\mathcal{PT}$ -antisymmetric soliton in the system with  $\delta = 0.4, \gamma = 0.3$  for  $k = 1.5$ . Components  $u$  and  $v$  of the stationary solution are shown in panels (a) and (b), respectively. (c) The spectrum of eigenvalues for small perturbations, including unstable ones. (d) The evolution of the soliton's  $u$ -component under the action of small random perturbations at the amplitude level of 1%. The evolution of the  $v$ -component is similar (not shown here).

corresponding to  $\geq 50$  diffraction (Rayleigh) lengths of the unperturbed soliton. The computation of the instability growth rate from the numerical solution of Eq. (29) produced results compatible with those obtained from the direct simulations (there may be a residual eigenvalue  $\sim 0.01$  close to the boundary, which does not give rise to any instability for long enough propagation distance in the simulations).

At  $\gamma = 0$ , the stability boundaries shown in Fig. 6 are identical to those presented in Ref. [40]. Naturally, the stability area shrinks with the increase of the gain-loss strength  $\gamma$ , and disappears at  $\gamma \approx 0.8$ , i.e., before reaching the exceptional point,  $\gamma = 1$ . Stability boundaries are not displayed for  $k < 1.14$ , as the solitons become very broad for such values, and convergence of the numerical iterations generating stationary solitons becomes very slow. The smallest value of  $k$  at which solitons were found is  $k \approx 1.04$ . Note that values of  $k$  in the bandgaps, at which solitons may exist, are bounded from below, as seen in Eq. (15).

## B. Dynamics of unstable solitons

For unstable solitons, the simulations make it possible to distinguish several dynamical scenarios. First, the collapse (blowup) is a generic scenario in the entire instability area, see, e.g., Fig. 4. Collapse may be avoided by unstable solitons residing close to the stability boundary. Namely, at relatively small values of  $\delta$  and  $\gamma$ , weak instability spontaneously transforms stationary solitons with a relatively small amplitude into breathers, as shown in Figs. 7(a,b). This outcome depends on the particular realization of small random perturbations applied to the soliton.

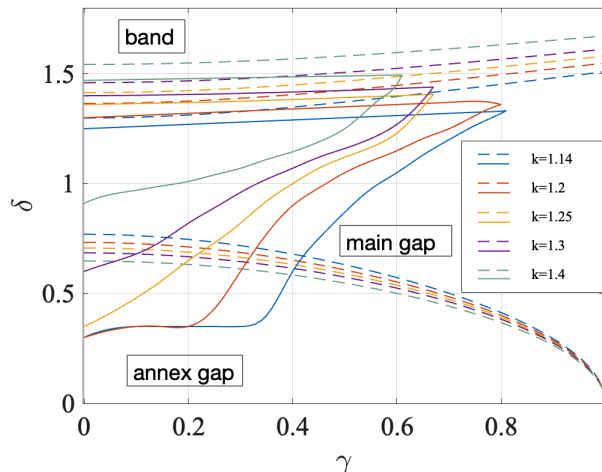


FIG. 6: (Color online). Families of solitons with indicated values of propagation constant  $k$  are stable in areas surrounded by the respectively colored solid curves, being unstable outside. Dashed curves of the same colors in the upper part of the panel correspond to  $\gamma = \gamma_{\text{SIG}}$ , see Eq. (17). They designate boundaries between the main (semi-infinite) gap and the band of linear waves, where solitons cannot exist. In the lower part, the dashed curves, which correspond to  $k = k_{\text{SIG}}$  (see Eq. (13)), indicate boundaries between the main and annex gaps.

Another realization initiates, instead, decay of the same soliton, as shown in Fig. 7(c,d). The blowup of the same unstable soliton is possible too, under the action of a different realization (not shown here). This peculiarity is possible because an unstable soliton may give rise to several different unstable eigenvalues, associated with different eigenmodes of small perturbations (see, e.g., Fig. 4(b)). Accordingly, a specially crafted small initial perturbation may excite a specific eigenmode.

At larger values of  $\gamma$  and  $\delta$ , it may also happen that an unstable soliton is not destroyed. Instead, as shown in Figs. 8(c,d), the perturbed soliton starts spontaneous motion with weak vibrations (actually, it develops a tilt in the spatial domain). The size of the tilt (“velocity”) depends on both a particular realization of the small random perturbation applied to the soliton and the system’s parameters. The inversion of the sign of the  $\mathcal{PT}$  coefficient,  $\gamma \rightarrow -\gamma$ , produces the same result, but with the opposite sign of the tilt. This observation is explained by the ( $\mathcal{PT}$ ) invariance of the underlying equations (1) and (2) with respect to substitution

$$(u, v) \rightarrow (u^*, v^*), z \rightarrow -z, \gamma \rightarrow -\gamma, \quad (40)$$

if it is applied to Eq. (5).

Lastly, it is relevant to mention that, under the action of the above-mentioned regularizing effect provided by SOC, Eqs. (7) and (8) produce stationary solitons solutions at  $\gamma > 1$ , while it is usually assumed that solitons cannot exist beyond the exceptional point (in particular, the exact solution given by Eqs. (22)-(24) for  $\delta = 0$  does not exist at  $\gamma > 1$ ). Indeed, Eq. (13) defines a formal bandgap also for  $\gamma > 1$ , although a part of the spectrum is complex in this case, see Eq. (11). An example of the soliton found at  $\gamma = 1.2$  is displayed in Figs. 9(a,b). As expected, it is unstable against spontaneous onset of the blowup, see Figs. 9(c,d). Nevertheless, it is relevant to stress that this is a genuine solution of Eqs. (7) and (8), rather than the so-called “ghost state”, which may be found as a formal solution beyond the exceptional point, but does not represent a true stationary state of the system [58, 59].

### C. Interactions between solitons

The availability of stable solitons suggests a possibility to explore interactions between them, initially placing two solitons at some distance  $d$  between their centers (this possibility was not explored in work [40], which introduced the conservative system with  $\gamma = 0$ ). It is well known that, in usual conservative models, pairs of well separated in-phase and out-of-phase solitons (ones with phase difference  $\Delta\phi = 0$  or  $\pi$ ) feature, respectively, mutual attraction or repulsion [60]. In our system, a qualitatively similar situation is exhibited by Fig. 10, where  $d = 10$ , while the FWHM width of each soliton is  $\simeq 1.5$ . In Figs. 10(a,b), two in-phase solitons originally attract each other, then bounce back twice, still keeping a considerable distance, and eventually separate. The essentially complex intrinsic structure of

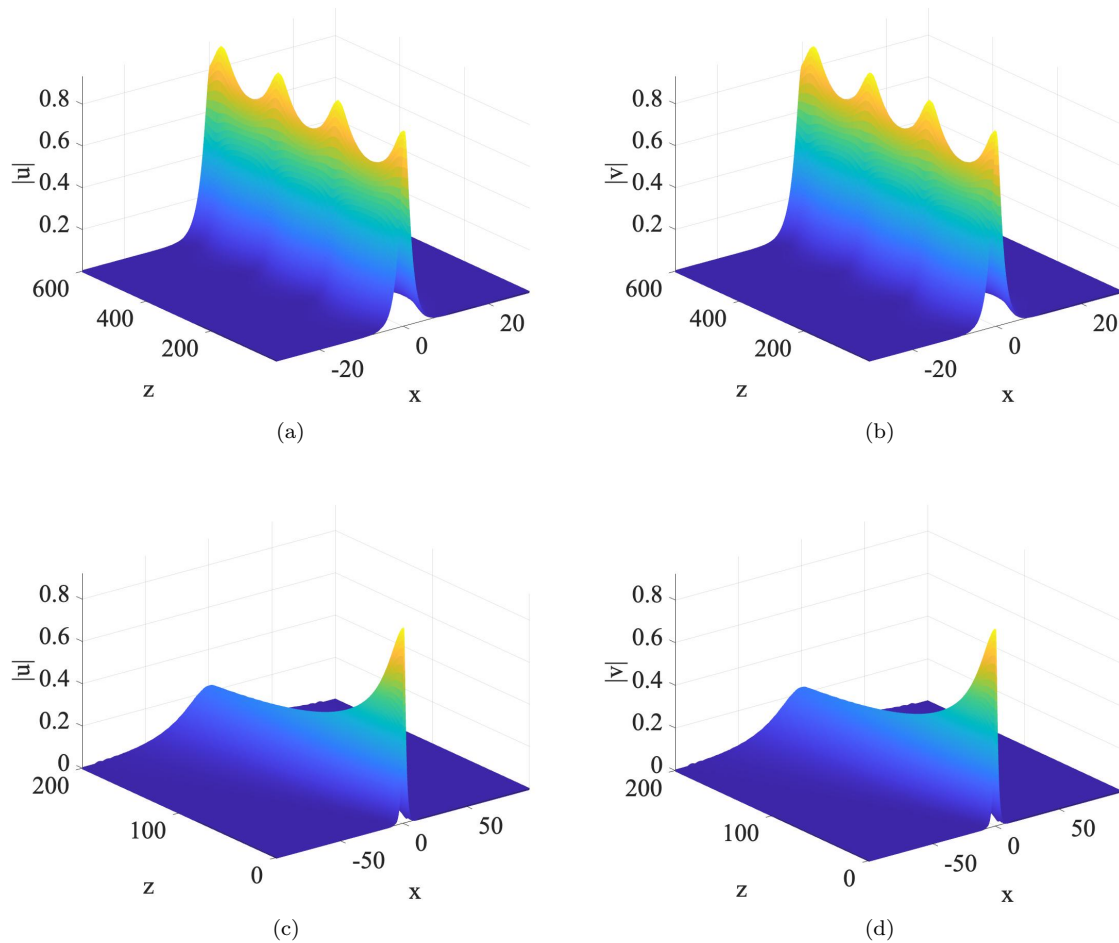


FIG. 7: (Color on line). Long-time evolution of a weakly unstable soliton at  $\delta = 0.35, \gamma = 0.1$ , with propagation constant  $k = 1.25$ . The simulations were initiated with random perturbations at the amplitude level of 1% added to the stationary soliton. Depending on the particular realization of the random perturbation, three different outcomes of the evolution are possible: transformation into a breather in (a,b); decay in (c,d); and blowup (not shown here).

solitons governed by Eqs. (1) and (2) leads to the change of the initial phase shift between the interacting solitons, leading to the fact that eventually separating solitons develop a phase shift of  $\pi$ . In Figs. 10(c,d), the simulation demonstrates straightforward repulsion and separation of the same pair of the stable solitons, but with the initial phase shift  $\Delta\phi = \pi$ .

The interaction is more complex for the same pair of solitons with a smaller initial separation, such as  $d = 6$  in Fig. 11. In this case, the original overlap between the solitons is conspicuous, which does not allow to consider them as a usual separated pair. As a result, the character of the interaction is drastically different from the usual pattern: as shown in Figs. 11(a,b), the in-phase solitons immediately *repel* each other, while the out-of-phase solitons feature *attraction*. In the latter case, they eventually merge into a single object, which is then destroyed by the blow-up (collapse).

#### D. Tilted (“moving”) solitons

The study of tilted (moving) solitons in the presence of SOC is a nontrivial issue, as SOC (unlike the gain and loss terms which represent the  $\mathcal{PT}$  symmetry) destroys the system’s Galilean invariance, making it impossible to construct moving solitons as boosted copies of quiescent ones. In Ref. [40], the analysis of the solutions in the tilted (“moving”) reference frame, with  $x$  replaced by the tilted coordinate (20), had demonstrated that all tilted solitons in the conservative system with  $\gamma = 0$  are unstable. In most cases, it is weak instability, which spontaneously transforms

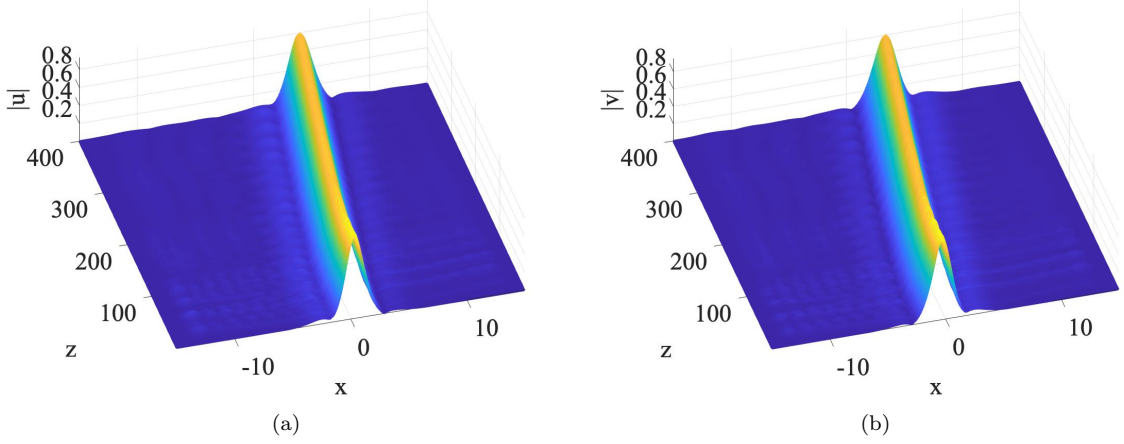


FIG. 8: (Color on line). The evolution of a weakly unstable soliton at  $\delta = 1, \gamma = 0.6$ , with propagation constant  $k = 1.14$ . The simulations were initiated with random perturbations at the amplitude level of 1% added to the stationary soliton, which is located close to the stability boundary for  $k = 1.14$ , see Fig. 2. The soliton spontaneously develops tilt in the spatial domain (“motion”). The change of the sign of  $\gamma$  leads to a similar result with the opposite sign of the tilt.

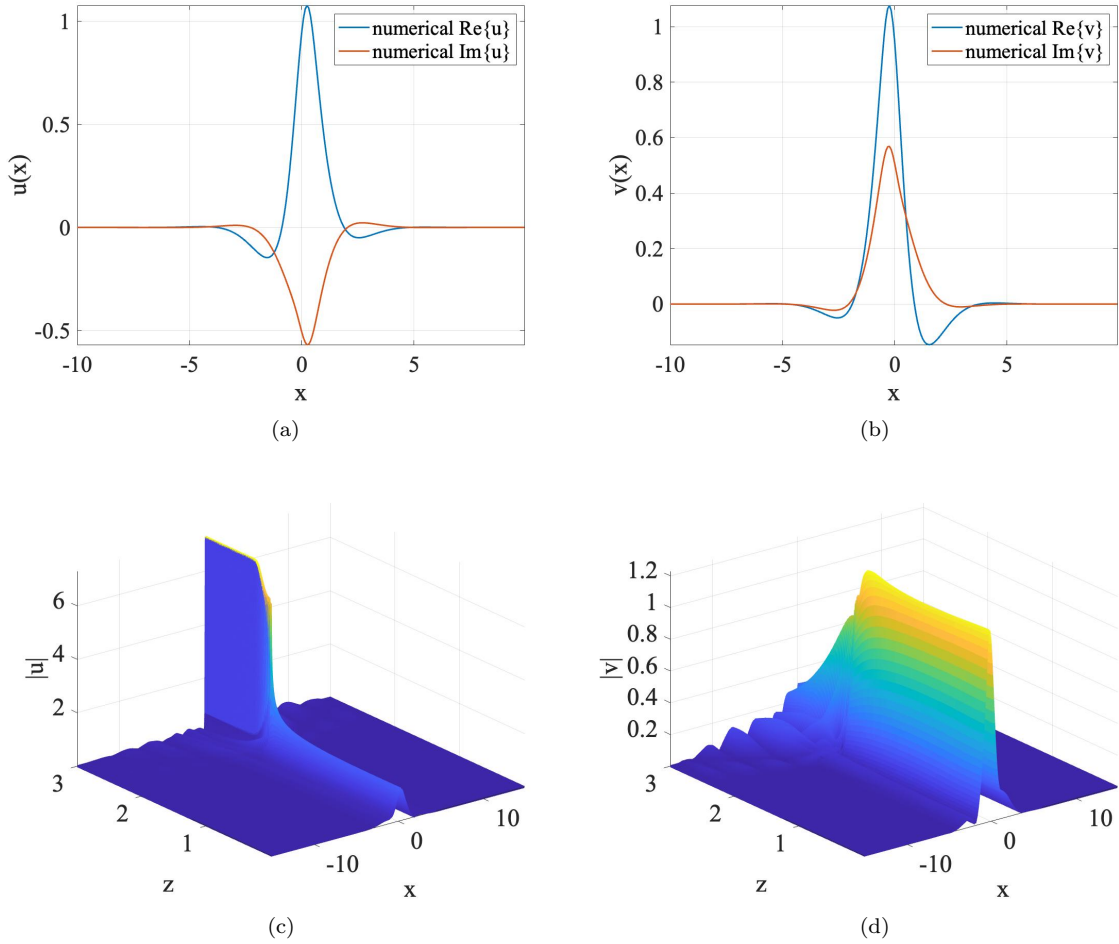


FIG. 9: (Color online). (a,b): An example of an unstable soliton found, as a numerical solution of Eqs. (7) and (8), at  $\gamma = 1.2$ , i.e., beyond the exceptional point ( $\gamma = 1$ ). Other parameters of the soliton are  $\delta = 1$  and  $k = 1.2$ . Panels (c) and (d) demonstrate instability of this state against spontaneous onset of the blowup.

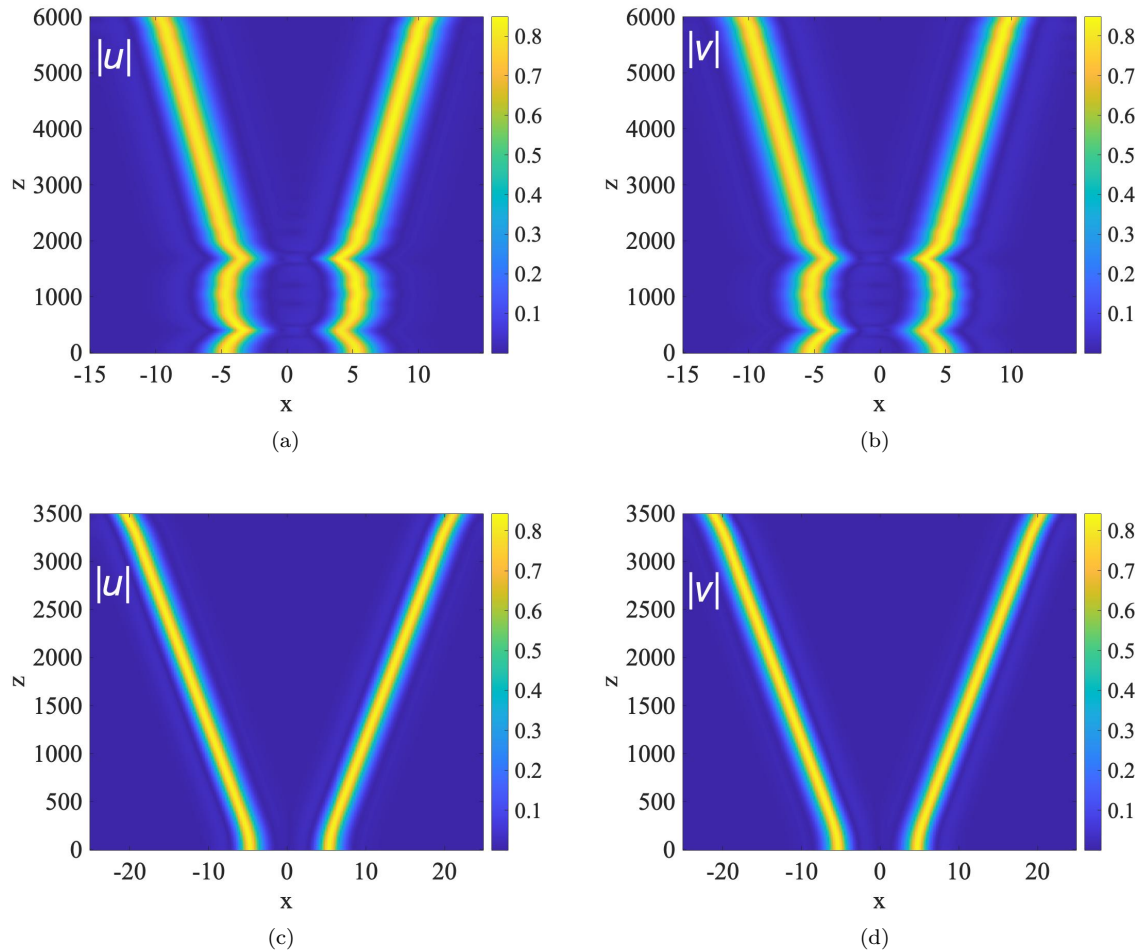


FIG. 10: (Color on line). Simulations of the interaction of two stable solitons with parameters  $\delta = 1, \gamma = 0.1$  and  $k = 1.2$ , initially separated by distance  $d = 10$ . (a,b): Relatively complex interaction of the in-phase solitons, with the initial phase shift  $\Delta\phi = 0$ . (c,d): Straightforward repulsion between the out-of-phase solitons, with  $\Delta\phi = \pi$ .

the tilted solitons into breathers. In the present system, which includes the gain-and-loss terms, systematic simulations also produce unstable tilted solitons. At small values of the tilt, such as  $c = 0.2$  in Fig. 12, the instability is relatively weak. With “favorable” realizations of random perturbations, a tilted soliton is spontaneously converted into a robust tilted breather, as shown in Figs. 12(a,b). Note that the established amplitude of the breather is essentially higher than that of the input soliton, which implies that the formation of such an “enhanced” breather may be considered as an “arrested collapse”. On the other hand, similar to what is shown above for quiescent unstable solitons in Fig. 7, “unfavorable” perturbations may initiate decay of the same soliton, as is seen in Figs. 12(c,d). At large  $c$ , unstable solitons always suffer destruction (not shown here in detail).

### E. Unstable solitons in the reduced system

Similar to the conservative system ( $\gamma = 0$ ) considered in Ref. [40] (see also the exact solution (36)), the simplified system of Eqs. (30) and (31), which neglects the paraxial diffraction, can readily produce soliton solutions in the finite bandgap (38), but they all turn out to be unstable, on the contrary to the above results (families of stable solitons in the SIG and AG) produced for the full system of Eqs. (1) and (2). A typical example of an unstable soliton generated by the reduced system, along with the spectrum of its (in)stability eigenvalues and results of the perturbed evolution, which shows destruction of the soliton, is displayed in Fig. 13.

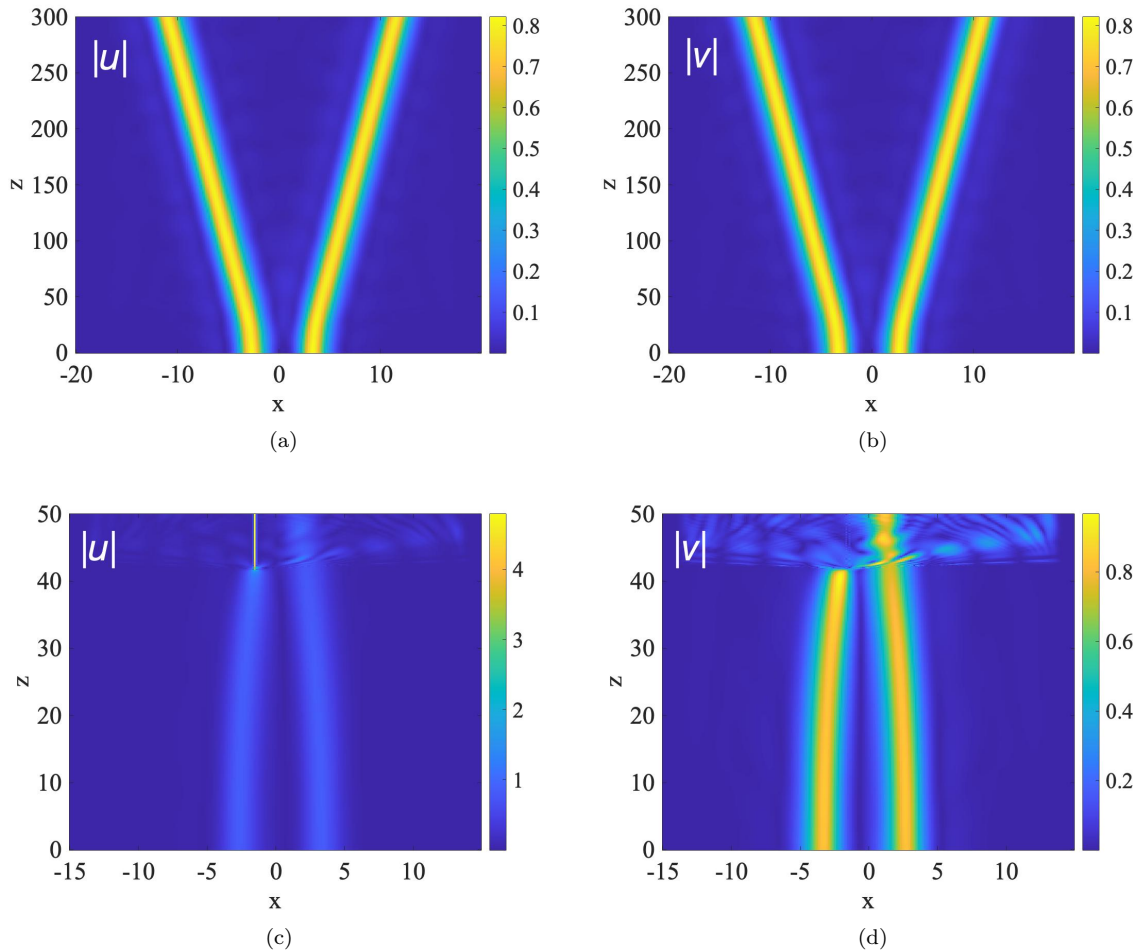


FIG. 11: (Color on line). The evolution of the same pairs of solitons as in Fig. 10, but with a smaller initial separation,  $d = 6$ . In panels (a) and (b), the in-phase solitons, counter-intuitively, repel each other. In panels (c) and (d), out-of-phase solitons unexpectedly exhibit attraction, and eventually merge into an collapsing state.

#### IV. CONCLUSION

In this work we have introduced the 1D system which blends the  $\mathcal{PT}$ -symmetry, emulated SOC, and quintic (critical) nonlinearity. The system is designed as a dual-core optical waveguide with skewed coupling between the cores. The scheme makes it possible to produce families of stable solitons in a very “precarious” situation, as both the combination of the gain and loss terms in the parallel waveguiding cores, which represents the  $\mathcal{PT}$ -symmetry, and the critical self-focusing make the solitons prone to the blowup instability. Nevertheless, the effective SOC, which is represented by terms mixing the fields in the cores through linear terms with the first spatial derivatives, added to the usual (straight) linear coupling, turn out to be strong enough to stabilize parts of the soliton families, which are found in both the main SIG (semi-infinite gap) and the finite AG (annex gap), adjacent to the SIG. As concerns unstable solitons, several scenarios of their evolution have been identified. In addition to the generic blowup, weak instability may transform the solitons into robust breathers. Interestingly, due to the regularizing effect exerted by SOC on the system’s instability beyond the point of the breakup of the  $\mathcal{PT}$  symmetry, stationary solitons are found in this case too, although they are unstable. Simulations of interactions between adjacent solitons have revealed both repulsion between them and merger into a collapsing mode.

As an extension of the analysis, it may be relevant to consider effects of spatial inhomogeneity, if it is present in the system. In particular, the  $\mathcal{PT}$ -symmetric gain-loss terms may be made inhomogeneous, representing a spatially odd imaginary potential [5]. It may be also interesting to develop the analysis for systems with fractional diffraction [61, 62], and for systems including a trapping potential [63, 64], as well as for periodic waves [65]. Another possibility may be to apply machine-learning techniques to these systems [66].

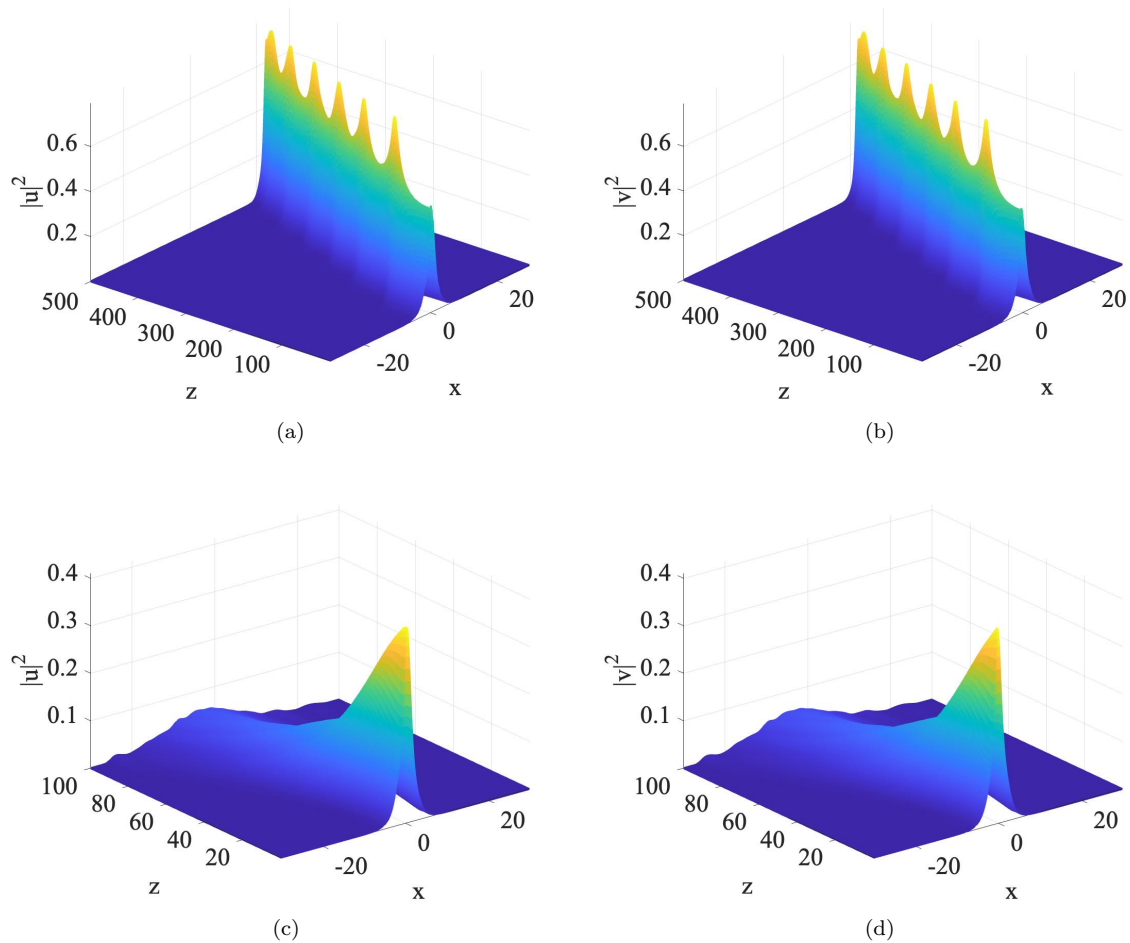


FIG. 12: (Color on line). The perturbed evolution of unstable tilted solitons with “velocity”  $c = 0.2$  (see Eq. (20)) and propagation constant  $k = 1.3$ , in the system with  $\delta = 1.2$  and  $\gamma = 0.2$ . In panels (a) and (b), the soliton transforms itself into an enhanced (relatively tall) robust breather. In (c) and (d), an “unfavorable” realization of the random perturbation initiates decay of the soliton.

### Declaration of Competing Interest

The authors declare that they have no known competing financial interests or personal relationships that could have appeared to influence the work reported in this paper.

### CRediT authorship contribution statement

Gennadiy Burlak: Numerical simulations, Data analysis, Manuscript drafting. Zhaopin Chen: Development of numerical methods, Numerical simulations, Data analysis, Manuscript drafting. Boris A. Malomed: Conceptualization, Analytical considerations, Data analysis, Manuscript drafting and editing.

### Acknowledgments

This work was supported, in part, by the Israel Science Foundation through grant No. 1286/17 and, in part, by the CONACYT (México) through grant No. A1-S-9201. Z.C. acknowledges a fellowship provided by the Helen Diller

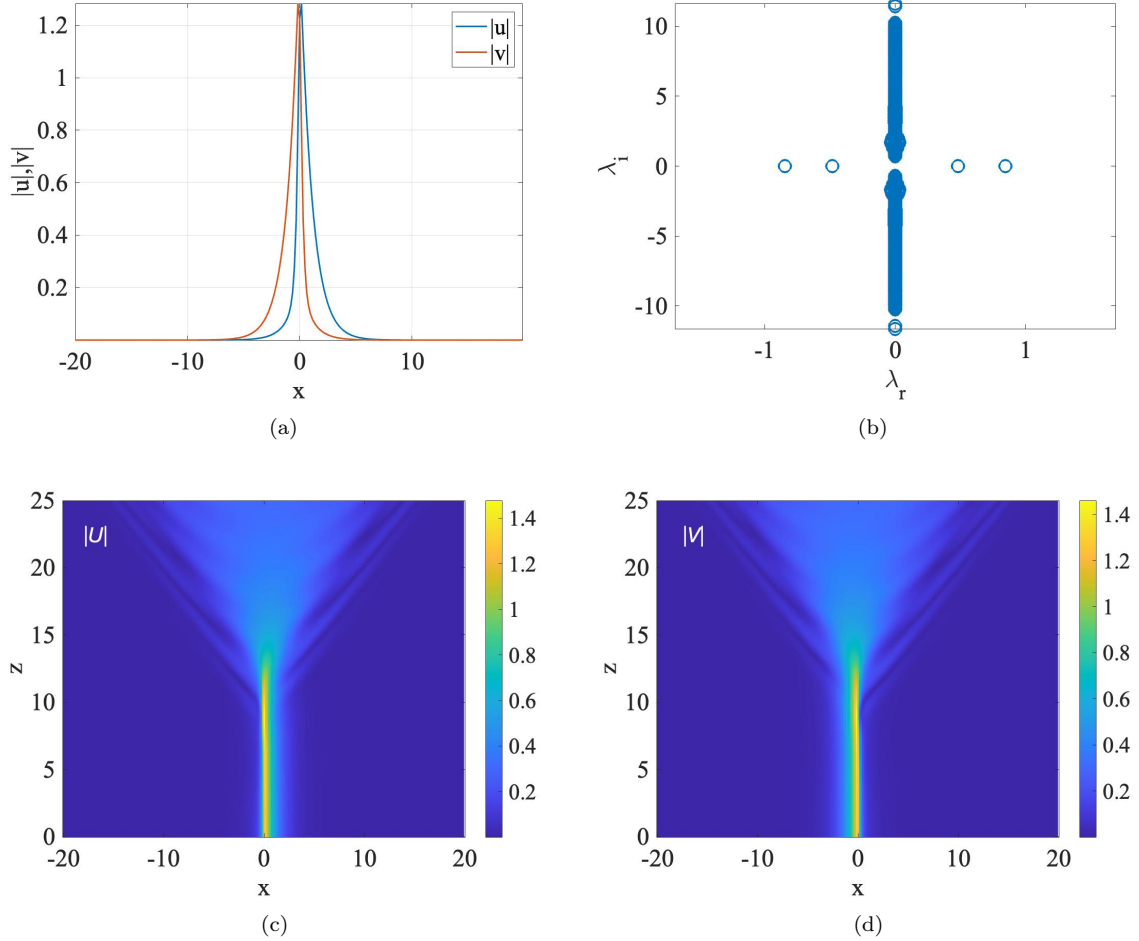


FIG. 13: (Color on line). A typical example of an unstable soliton produced by the reduced system of Eqs. (30), (31) with  $\gamma = 0.2$ . The soliton's propagation constant is  $k = -0.2$ . (a) The structure of the soliton; (b) the eigenvalue spectrum, which includes two pairs of unstable modes of small perturbations; (c,d) the evolution of the soliton under the action of random perturbations initially added at the 1% amplitude level.

quantum center at the Technion (Haifa, Israel).

- 
- [1] Longhi S. Quantum-optical analogies using photonic structures. *Laser & Photon. Rev.* 2009;3:243-261.
  - [2] Leyder C, Romanelli M, Karr JP, Giacobino E, Liew T CH, Glazov MM, Kavokin AV, Malpuech G, Bramati A. Observation of the optical spin Hall effect. *Nature Phys.* 2007;3:628–631.
  - [3] Rechtsman MC, Zeuner JM, Plotnik Y, Lumer Y, Podolsky D, Dreisow F, Nolte S, Segev M, Szameit A. Photonic Floquet topological insulators. *Nature* 2013;496:196-200.
  - [4] Leonhardt U, Piwnicki P. Optics of nonuniformly moving media. *Phys. Rev. A* 1999;60:4301
  - [5] Bender CM. Rep. Making sense of non-Hermitian Hamiltonians. *Prog. Phys.* 2007;70:947.
  - [6] Ruschhaupt A, Delgado F and Muga JG. Physical realization of-symmetric potential scattering in a planar slab waveguide. *J. Phys. A: Math. Gen.* 2005;38:L171.
  - [7] El-Ganainy R, Makris KG, Christodoulides DN, Musslimani ZH. Theory of coupled optical  $\mathcal{PT}$ -symmetric structures. *Opt. Lett.* 2007;32:2632.
  - [8] Berry MV J. Optical lattices with  $\mathcal{PT}$  symmetry are not transparent. *Phys. A: Math. Theor.* 2008;41:244007.
  - [9] Klaiman S, Günther U, Moiseyev N. Visualization of Branch Points in  $\mathcal{PT}$ -Symmetric Waveguides. *Phys. Rev. Lett.* 2008;101:080402.
  - [10] Longhi S. Bloch Oscillations in Complex Crystals with Symmetry. *Phys. Rev. Lett.* 2009;103:123601.
  - [11] Makris KG, El-Ganainy R, Christodoulides DN, Musslimani ZH.  $\mathcal{PT}$ -Symmetric Periodic Optical Potentials. *Int. J. Theor.*

- Phys. 2011;50:1019.
- [12] Suchkov SV, Sukhorukov AA, Huang J, Dmitriev SV, Lee C, Kivshar YS. Nonlinear switching and solitons in  $\mathcal{PT}$ -symmetric photonic. *Laser Photonics Rev.* 2016;10:177.
  - [13] Konotop VV, Yang J, Zezyulin DA, Nonlinear waves in  $\mathcal{PT}$ -symmetric systems. *Rev. Mod. Phys.* 2016;88:035002.
  - [14] Guo A, Salamo GJ, Duchesne D, Morandotti R, Volatier-Ravat M, Aimez V, Siviloglou GA, Christodoulides DN. Observation of  $\mathcal{PT}$ -symmetry breaking in complex optical potentials. *Phys. Rev. Lett.* 2009;103:093902.
  - [15] Rüter CE, Makris KG, El-Ganainy R, Christodoulides DN, Segev M, Kip D. Observation of parity–time symmetry in optics. *Nature Phys.* 2010;6:192-195.
  - [16] Regensburger A, Bersch C, Miri M-A, Onishchukov G, Christodoulides DN, Peschel U. Parity–time synthetic photonic lattices. *Nature* 2012;488:167-171.
  - [17] Bliokh KY, Rodriguez-Fortuno FJ, Nori F, Zayats AV. Spin–orbit interactions of light. *Nature Photon.* 2015;9:796.
  - [18] Kartashov YV, Malomed BA, Konotop VV, Lobanov VE, Torner L. Stabilization of solitons in bulk Kerr media by dispersive coupling. *Opt Lett* 2015;40:1045-1048.
  - [19] Sakaguchi H, Malomed BA. One- and two-dimensional solitons in  $\mathcal{PT}$ -symmetric systems emulating spin-orbit coupling. *New J. Phys.* 2016;18:105005.
  - [20] Lin YJ, Jimenez-Garcia K, Spielman I. Spin-orbit-coupled bose-einstein condensates. *Nature* 2011;471:83-6.
  - [21] Galitski V, Spielman I B. Spin–orbit coupling in quantum gases. *Nature* 2013;494:49.
  - [22] Goldman N, Juzeliūnas G, Öhberg P, Spielman IB. Light-induced gauge fields for ultracold atoms. *Rep. Prog. Phys.* 2014;77:126401.
  - [23] Zhai H. Degenerate quantum gases with spin–orbit coupling: a review. *Rep. Prog. Phys.* 2015;78:026001.
  - [24] Malomed BA. Creating solitons by means of spin-orbit coupling. *EPL* 2018;122:3600.
  - [25] Wu MW, Jiang JH, Weng MQ. Spin dynamics in semiconductors. *Phys. Rep.* 2010;493:61-236.
  - [26] Manchon A, Koo, HC, Nitta J, Frolov SM, Duine RA. New perspectives for Rashba spin-orbit coupling. *Nature Materials* 2015;14:871-882.
  - [27] Ding K, Ma GC, Xiao M, Zhang ZQ, Chan CT. Emergence, coalescence, and topological properties of multiple exceptional points and their experimental realization. *Phys. Rev. X* 2016;6:021007.
  - [28] Miri MA, Alù A. Exceptional points in optics and photonics. *Science* 2019;363:43.
  - [29] Ozdemir SK, Rotter S, Nori F, Yang L. Parity-time symmetry and exceptional points in photonics. *Nature Materials* 2019;18:783-798.
  - [30] Wright EM, Stegeman GI and Wabnitz S. Solitary-wave decay and symmetry-breaking instabilities in two-mode fibers. *Phys. Rev. A* 1989;40:4455.
  - [31] Romagnoli M, Trillo S, Wabnitz S. Soliton switching in nonlinear couplers. *Opt. Quantum Electron.* 1992;24:S1237–S1267.
  - [32] Malomed BA. A variety of dynamical settings in dual-core nonlinear fibers. In: *Handbook of Optical Fibers, Vol. 1*, pp. 421-474 (G.-D. Peng, Editor: Singapore: Springer, 2019).
  - [33] Driben R, Malomed BA. Stability of solitons in parity-time-symmetric couplers. *Opt. Lett.* 2011;36:4323-4325.
  - [34] Driben R, Malomed BA. Stabilization of solitons in  $\mathcal{PT}$  models with supersymmetry by periodic management. *EPL* 2011;96:51001.
  - [35] Alexeeva NV, Barashenkov IV, Sukhorukov AA, Kivshar YS. Optical solitons in  $\mathcal{PT}$ -symmetric nonlinear couplers with gain and loss. *Phys. Rev. A* 2012;85:063837.
  - [36] Burlak G, Malomed BA. Stability boundary and collisions of two-dimensional solitons in  $\mathcal{PT}$ -symmetric couplers with the cubic-quintic nonlinearity. *Phys. Rev. E* 2013;88:062904.
  - [37] Chen Z, Liu J, Fu S, Li Y, Malomed BA. Discrete solitons and vortices on two-dimensional lattices of  $\mathcal{PT}$ -symmetric couplers. *Opt Express* 2014;22(24):29679-92.
  - [38] Burlak G, Garcia-Paredes S, Malomed BA.  $\mathcal{PT}$ -symmetric couplers with competing cubic-quintic nonlinearities. *Chaos* 2016;26:113103.
  - [39] Fan Z and Malomed BA. Dynamical control of solitons in a parity-time-symmetric coupler by periodic management. *Comm. Nonlin. Sci. Num. Sim.* 2019;79:104906.
  - [40] Shamriz E, Chen Z, and Malomed BA. Stabilization of one-dimensional Townes solitons by spin-orbit coupling in a dual-core system. *Comm. Nonlin. Sci. Num. Sim.* 2020;91:105412.
  - [41] Bergé L. Wave collapse in physics: principles and applications to light and plasma waves. *Phys. Rep.* 1998;303:259–372.
  - [42] Sulem C, Sulem PL. *The Nonlinear Schrödinger Equation: Self-Focusing and Wave Collapse.* New York: Springer; 1999.
  - [43] Fibich G. *The nonlinear Schrödinger equation: singular solutions and optical collapse.* Heidelberg: Springer; 2015.
  - [44] Chiao RY, Garmire E, Townes CH. Self-trapping of optical beams. *Phys. Rev. Lett.* 1964;13:479–82.
  - [45] Abdullaev FK, Salerno M. Gap-townes solitons and localized excitations in low-dimensional Bose-Einstein condensates in optical lattices. *Phys. Rev. A* 2005;72:033617.
  - [46] Senthilnathan K, Li Q, Nakkeeran K, Wai PKA. Robust pedestal-free pulse compression in cubic-quintic nonlinear media. *Phys. Rev. A* 2008;78:033835.
  - [47] Mihalache D, Mazilu D, Crasovan LC, Towers I, Malomed BA, Buryak AV, Torner L, Lederer F. Stable three-dimensional spinning optical solitons supported by competing quadratic and cubic nonlinearities. *Phys. Rev. E* 2002;66:13.
  - [48] Mardonov S, Sherman EY, Muga JG, Wang HW, Ban Y, Chen, X. Collapse of spin-orbit-coupled Bose-Einstein condensates. *Phys. Rev. A.* 2015;91:043604.
  - [49] Sakaguchi H, Li B, Malomed BA. Creation of two-dimensional composite solitons in spin–orbit-coupled self-attractive Bose–Einstein condensates in free space. *Phys. Rev. E* 2014;89:032920.

- [50] Reyna AS, de Araújo CB. High-order optical nonlinearities in plasmonic nanocomposites – a review. *Adv. Opt. Phot.* 2017;9:720-774.
- [51] Alexeeva NV, Barashenkov IV, Saxena A. Spinor solitons and their  $\mathcal{PT}$ -symmetric offspring. *Annals of Physics* 2019;403:198-223.
- [52] Yang J and Lakoba T I, Accelerated imaginary-time evolution methods for the computation of solitary waves. *Stud. Appl. Math.* 2008;120:265292.
- [53] Yang J. *Nonlinear Waves in Integrable and Non-integrable Systems* (SIAM, Philadelphia, 2010).
- [54] Barashenkov IV, Zemlyanaya EV. Existence threshold for the AC-driven damped nonlinear Schrödinger solitons. *Physica D* 1999;132:363-372.
- [55] Barashenkov IV, Woodford SR. Complexes of stationary domain walls in the resonantly forced Ginsburg-Landau equation. *Phys. Rev. E* 2005;71:026613.
- [56] Barashenkov IV, Zemlyanaya EV. Travelling solitons in the externally driven nonlinear Schrödinger equation. *J. Phys. A: Math. Theor.* 2011;44:465211.
- [57] Alexeeva NV, Barashenkov IV, Kivshar YC. Solitons in  $\mathcal{PT}$ -symmetric ladders of optical waveguides. *New J. Phys.* 2017;19:113032.
- [58] Cartarius H, Haag D, Dast D, and Wunner G. Nonlinear Schrödinger equation for a  $\mathcal{PT}$ -symmetric delta-function double well. *J. Phys. A: Math Theor.* 2012;45:444008.
- [59] Susanto H, Kusdiantara R, Li N, Kirikchi OB, Adzkiya D, Putri ERM, Asfihani T. Snakes and ghosts in a parity-time-symmetric chain of dimers. *Phys. Rev. E* 2018;97:062204.
- [60] Kivshar YS and Malomed BA. Dynamics of solitons in nearly integrable systems. *Rev. Mod. Phys.* 1989;61:763-915.
- [61] Malomed BA. Optical solitons and vortices in fractional media: A mini-review of recent results. *Photonics* 2021;8:353.
- [62] Cao QH, Dai CQ. Symmetric and anti-symmetric solitons of the fractional second- and third-order nonlinear Schrödinger equation. *Chin. Phys. Lett.* 2021;38:090501.
- [63] Raghuraman PJ, Baghya Shree S, Mani Rajan MS. Soliton control with inhomogeneous dispersion under the influence of tunable external harmonic potential. *Waves in Random Media* 2019;31:474-485.
- [64] Dai CQ, Wang YY, Zhang JF. Managements of scalar and vector rogue waves in a partially nonlocal nonlinear medium with linear and harmonic potentials. *Nonlinear Dynamics* 2020;102:379-391.
- [65] Dai CQ, Wang YY. Coupled spatial periodic waves and solitons in the photovoltaic photorefractive crystals. *Nonlinear Dynamics* 2020;102:1733-1741.
- [66] Fang Y, Wu G-Z, Wang YY, Dai CQ, Data-driven femtosecond optical soliton excitations and parameters discovery of the high-order NLSE using the PINN, *Nonlinear Dynamics* 2021;105:603-616.